Improving the Calibration of Type Ia Supernovae Using Late-time Lightcurves

Yun Wang, and Nicholas Hall

Homer L. Dodge Department of Physics & Astronomy
Univ. of Oklahoma, 440 W Brooks St., Norman, OK 73019
email: wang@nhn.ou.edu, nrhall@ucdavis.edu

ABSTRACT

The use of Type Ia supernovae (SNe Ia) as cosmological standard candles is key to solving the mystery of dark energy. Improving the calibration of SNe Ia increases their power as cosmological standard candles. We find tentative evidence for a correlation between the late-time lightcurve slope and the peak luminosity of SNe Ia; brighter SNe Ia seem to have shallower lightcurve slopes between 100-150 days from maximum light. Using a Markov Chain Monte Carlo (MCMC) analysis in calibrating SNe Ia, we are able to simultaneously take into consideration the effect of dust extinction, the luminosity and lightcurve width correlation (parametrized by Δm_{15}), and the luminosity and late-time lightcurve slope correlation. For the available sample of 11 SNe Ia with well-measured late-time lightcurves, we find that correcting for the correlation between luminosity and late-time lightcurve slope of the SNe Ia leads to an intrinsic dispersion of 0.12 mag in the Hubble diagram. Our results have significant implications for future supernova surveys aimed to illuminate the nature of dark energy.

Subject headings: distance scale – methods: data analysis – supernovae: general

1. Introduction

One of the most important problems in cosmology today is to solve the mystery of dark energy, the unknown reason for the observed cosmic acceleration (Riess et al. 1998; Perlmutter et al. 1999). The discovery of cosmic acceleration was made using Type Ia Supernovae (SNe Ia), as SNe Ia can be calibrated to be good cosmological standard candles (Phillips 1993; Riess, Press, & Kirshner 1995). Improving the calibration of SNe Ia increases their power as cosmological standard candles.

A SN Ia is a thermonuclear explosion that completely destroys a carbon/oxygen white dwarf as it approaches the Chandrasekher limit of 1.4 $M_{\odot}$.[1] This is the reason SNe Ia are so uniform in peak luminosity. The first challenge to overcome when using SNe Ia as cosmological standard candles is properly incorporating the intrinsic scatter in SN Ia peak luminosity. The usual calibration of SNe Ia reduces the intrinsic scatter in SN Ia peak luminosity to about 0.17 mag (Phillips 1993; Riess, Press, & Kirshner 1995). The calibration techniques used so far are based on one observable parameter, the lightcurve width, which can be parametrized either as Δm_{15} (decline in magnitudes in the B-band for a SN Ia in the first 15 SN Ia restframe days after B-band maximum, see Phillips (1993)), or a stretch factor (which linearly scales the time axis, see Goldhaber et al. (2001)). The lightcurve width is associated with the amount of ^{56}Ni produced in the SN Ia explosion, which in turn depends on when the carbon burning makes the transition from turbulent deflagration to a supersonic detonation (Wheeler 2003).

There are theoretical reasons to expect the existence of additional physical parameters that characterize the lightcurve of a SN Ia. For example, Milne, The, & Leising (2001) modeled the late light curves of SNe Ia, and found that the nonlocal and time-dependent energy deposition due to the transport of Comptonized electrons can produce a 0.10 to 0.18 mag correction to the late-time brightness of a SN Ia, depending on their position in the Δm_{15} sequence.

In this paper we show that late-time lightcurves of SNe Ia can be used to tighten the calibration of SNe Ia, and reduce their effective (post-calibration) intrinsic scatter in the Hubble diagram. We describe our method in Sec.2, and present our results in Sec.3. We summarize and conclude in Sec.4.

2. Method

2.1. Defining the sample

We use the lightcurve fits obtained using the Joint SuperStretch code for SN Ia lightcurves (Wang et al. 2006) [2] to derive the lightcurve parameters (epoch and apparent magnitudes at maximum light and Δm_{15}). This is necessary for consistency in making color and Δm_{15} corrections.

---

[1]The exception recently found by Howell et al. (2006) is super-luminous and can be easily separated from the normal SNe Ia used for cosmology.

[2]The B and V lightcurves were fit using no secondary bump.

We select a sample of "normal" SNe Ia (from a total of 135 available) that satisfy the following requirements:

(1) $B_{max} - V_{max} \leq 0.5$;
(2) $0.015 < z < .1$;
(3) B lightcurve data extending beyond 100 days from maximum light.

The requirement of $B_{max} - V_{max} \leq 0.5$ selects the "Branch normal" SNe Ia (Vaughan et al. 1995; Branch 1998), which is standard in studying SNe Ia as cosmological standard candles. The requirement of $0.015 < z < .1$ selects SNe Ia which are nearby yet distant enough, such that they are not affected by peculiar velocities due to cosmic large scale structure that modifies the Hubble diagram of nearby standard candles (Wang, Spergel, & Turner 1998), which has the largest impact on the nearest SNe Ia (see, e.g., Zehavi et al. (1998); Cooray & Caldwell (2006); Hui & Greene (2006); Conley et al. (2007)).

This yields a sample of 13 SNe Ia. Of these, we exclude two more SNe: SN1999cc, and SN1993h. SN1999cc has only one data point in the B lightcurve between 40 to 100 days from maximum light, insufficient to determine a slope independent of the lightcurve model. For SN1993h, the late-time lightcurve slope appears to depend on the lightcurve model, due to the appearance of a small secondary peak in the lightcurve data at ~ 80 days from maximum light. For the final set of 11 SNe Ia, the B lightcurves are very close to a straight line at $\gtrsim 70$ days from maximum light in the SN Ia restframe.

Our final sample consists of 11 SNe Ia that have lightcurve data at $\gtrsim 100$ days from maximum light in the SN Ia restframe, and late-time lightcurve slopes independent of the lightcurve model. Table 1 lists the SNe Ia in our sample. We include all the data that are required to allow others to reproduce our results.

2.2. Fitting the Absolute Magnitudes

To convert observed apparent magnitudes to absolute magnitudes we assume a flat universe, with $\Omega_m = 0.3$, $\Omega_\Lambda = 0.7$, and $H_0 = 70\,\mathrm{km\,s^{-1}\,Mpc^{-1}}$. The B absolute magnitudes

$$M_B^{obs} \equiv B_{max} - \mu, \tag{1}$$

where B_{max} denotes the apparent magnitude at peak brightness in the B band, and the distance modulus μ is

$$\mu(z) = m - M = 5 \log\left[d_L(z)/10\,\mathrm{pc}\right]. \tag{2}$$

Table 1: Nearby SNe Ia with well defined late-time lightcurves.

SN name	z	B_{max}	ΔB_{max}	V_{max}	Δm_{15}	b_{lt}	reference
SN1990O	0.031	16.607	0.035	16.533	0.961	0.0160	Hamuy et al. (1996b)
SN1990T	0.040	17.454	0.086	17.537	1.298	0.0152	Hamuy et al. (1996b)
SN1990Y	0.039	17.674	0.306	17.494	1.217	0.0153	Hamuy et al. (1996b)
SN1992bc	0.020	15.207	0.009	15.207	0.960	0.0147	Hamuy et al. (1996b)
SN1993ag	0.050	18.298	0.026	18.081	1.382	0.0142	Hamuy et al. (1996b)
SN1997dg	0.033	17.143	0.033	17.117	1.281	0.0177	Jha et al. (2006)
SN1998ec	0.020	16.670	0.053	16.406	1.074	0.0164	Jha et al. (2006)
SN1998V	0.017	15.912	0.029	15.738	1.150	0.0163	Jha et al. (2006)
SN1999ef	0.038	17.524	0.117	17.418	1.055	0.0160	Jha et al. (2006)
SN2000dk	0.016	15.637	0.021	15.543	1.457	0.0136	Jha et al. (2006)
SN2000fa	0.022	16.026	0.051	16.055	1.140	0.0164	Jha et al. (2006)

For $z < 0.1$, the luminosity distance $d_L(z)$ is well approximated by

$$d_L(z) = \frac{cz}{H_0}\left[1 + \frac{1}{2}(1 - q_0)\, z\right], \tag{3}$$

with $q_0 = \Omega_m/2 - \Omega_\Lambda$. Since we are only considering very low redshift SNe Ia, our results are insensitive to the assumed cosmological model.

Without any corrections, the dispersion of the SNe Ia in our sample in the Hubble diagram is 0.35 mag (see Fig.5(a)). This is due to extinction by dust, as well as the intrinsic dispersion in the luminosities of SNe Ia due to the physical diversity of these objects (Woosley et al. 2007). Our goal is to model these effects phenomenologically using observational data, in order to calibrate SNe Ia into good standard candles.

According to Cardelli, Clayton, & Mathis (1989), due to dust extinction, all true B magnitudes differ from the observed B magnitudes by $\delta B \equiv B - B^{obs} = R_B\, \delta(B-V)$, where $\delta(B-V) \equiv (B-V) - (B-V)^{obs}$, and R_B is approximately constant. Following van den Bergh (1995), we use $\mathcal{R}$ to denote the color correction coefficient parametrizing the combined effects of dust extinction and intrinsic SN color variation. Assuming that $B_{max} - V_{max} = 0$ for unreddened SNe Ia (Phillips et al. 1999), the dust correction to M_B^{obs} is $\mathcal{R}E$, with $E = B_{max} - V_{max}$.

There is a well known correlation between SN Ia peak luminosity and Δm_{15}, the decline in brightness (in units of mag) 15 days (in the SN restframe) after peak brightness (Phillips

1993). Following Wang et al. (2006), we parametrize the Δm_{15} dependence of M_B^{obs} with a piecewise linear function, $\mathcal{D}(\Delta m_{15}) = \alpha\ (\Delta m_{15} - 1.1) + \alpha\prime\ |\Delta m_{15} - 1.1|$.

We use the Markov Chain Monte Carlo (MCMC) technique (see Neil (1993) for a review), illustrated for example in Lewis & Bridle (2002), in the likelihood analysis. The MCMC method scales approximately linearly in computation time with the number of parameters. The method samples from the full posterior distribution of the parameters, and from these samples the marginalized posterior distributions of the parameters can be estimated. In the MCMC analysis, we fit M_B^{obs} to

$$M_B^{fit} = M + \Delta M^{cor} = M + \mathcal{R}E + \alpha\ (\Delta m_{15} - 1.1) + \alpha\prime\ |\Delta m_{15} - 1.1| + \beta b_{lt}, \tag{4}$$

where b_{lt} (in units of mag/day) is the late-time lightcurve slope (in the SN restframe). In our MCMC code, we use

$$\chi^2 = \sum_{i=1}^{N} \left(\frac{M_B^{obs}(z_i) - M_B^{fit}(z_i)}{\Delta B_{max}(z_i)} \right)^2. \tag{5}$$

The MCMC algorithm allows us to explore the dependence of M_B^{obs} on all the parameters simultaneously.

The Hubble diagram dispersion is a conventional measure of the intrinsic scatter of SNe Ia; it is given by the standard deviation of the apparent magnitudes at maximum light of the SNe Ia, B_{max}, from the theoretical predictions given by

$$m_0(z) \equiv \mu(z) + M, \tag{6}$$

where M is a constant that denotes the absolute magnitude of SNe Ia; it can only be determined through direct measurements of the distances to the SNe Ia using Cepheid variable stars. Since M has no impact on the relative calibration of SNe Ia that we study in this paper, we allow M to vary in order to obtain the smallest scatter in the Hubble diagram, independent of the M values obtained in the MCMC likelihood analysis. This is the same approach adopted by Wang et al. (2006).

3. Results

We have used the restframe lightcurves to obtain slopes of the lightcurves at late-time, chosen to be between 100 and 150 days from maximum light. Since the lightcurves are very close to straight lines at $\gtrsim 70$ days from maximum light, the measured slopes are robust and not dependent on the lightcurve model. Table 1 lists the late-time lightcurve slopes b_{lt} for the SNe Ia in our sample.

Our data consist of (B_{max}, ΔB_{max}, E, Δm_{15}, b_{lt}) for each of the SNe Ia in our sample. The parameters that we vary in our MCMC likelyhood analysis are (M, $\mathcal{R}$, α, $\alpha\prime$, β). Wang et al. (2006) found that $\mathcal{R} = 2.59 \pm 0.24$, $\alpha = 0.78 \pm 0.09$, and $\alpha\prime = -0.54 \pm 0.19$. To avoid obtaining unphysical values of α and $\alpha\prime$ due to the small size of our sample, we impose a prior of $\alpha\prime \geq -2$ in our analysis.

We obtain millions of MCMC samples, which are then appropriately thinned for statistical independence. We do not present results on the "nuisance" parameters M; it is marginalized over in obtaining the probability distributions that we present. Fig.1 shows the marginalized probability density functions (pdf) of $\mathcal{R}$, α, $\alpha\prime$, and β. Fig.2 shows the corresponding 2-D joint confidence contours (68% and 95%) for these parameters. For comparison, Fig.3 and Fig.4 show the pdf and joint confidence contours for $\mathcal{R}$, α, and $\alpha\prime$, with $\beta = 0$. In Fig.1 and Fig.3, the dotted lines are the likelihood functions. Agreement between the pdf and the likelihood function indicates that the MCMC chains have converged and hence provide reliable pdf's. Table 2 lists the best fit, mean, and standard deviations for $\mathcal{R}$, α, $\alpha\prime$, β.

Table 2: Best fit, mean, and standard deviations for $\mathcal{R}$, α, $\alpha\prime$, β.

parameter	best fit	mean	rms dev
	including b_{lt}:		
$\mathcal{R}$	2.407	2.445	0.141
α	1.890	1.870	0.109
$\alpha\prime$	−1.453	−1.418	0.244
β	77.490	80.925	12.779
	not including b_{lt}	($\beta = 0$):	
$\mathcal{R}$	2.454	2.480	0.123
α	2.007	1.994	0.051
$\alpha\prime$	−2.000	−1.969	0.030

It is reassuring that we obtain the same value of $\mathcal{R}$ whether or not we include late-time lightcurve slope b_{lt} in our analysis. Note that the prior of $\alpha\prime \geq -2$ has little impact if we include b_{lt} in our analysis (see Figs.1-2), but it has a very large impact if we only fit for (M, $\mathcal{R}$, α, $\alpha\prime$). This indicates that the set of parameters (M, $\mathcal{R}$, α, $\alpha\prime$) does not properly describe the data, given reasonable physical priors on $\alpha\prime$.

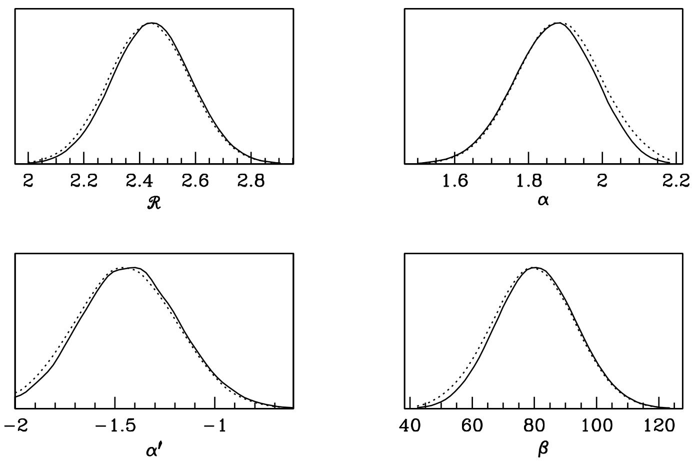

Fig. 1.— Marginalized probability density functions (pdf) of $\mathcal{R}$, α, $\alpha\prime$, and β.

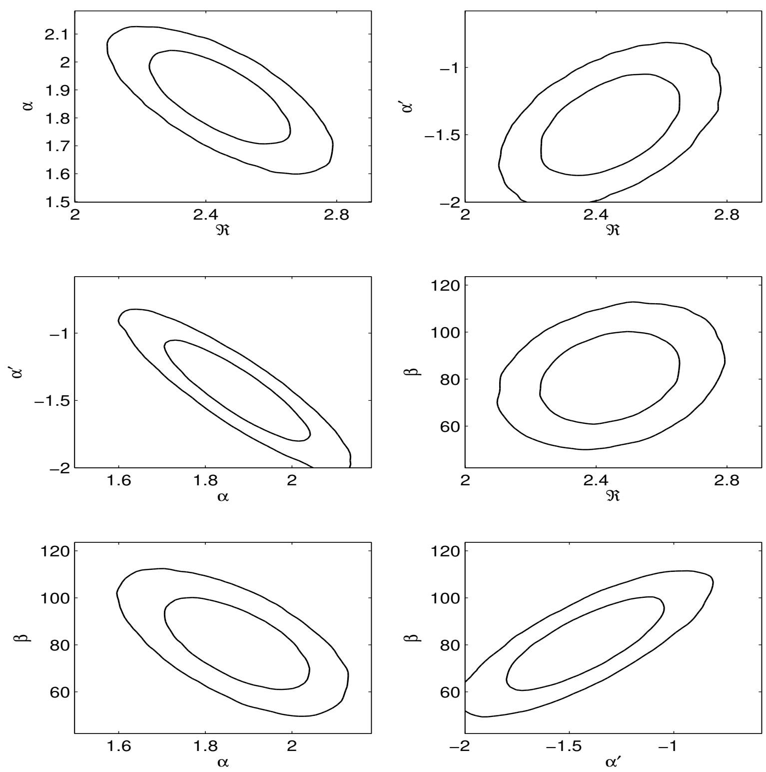

Fig. 2.— 2-D joint confidence level contours (68% and 95%) corresponding to Fig.1.

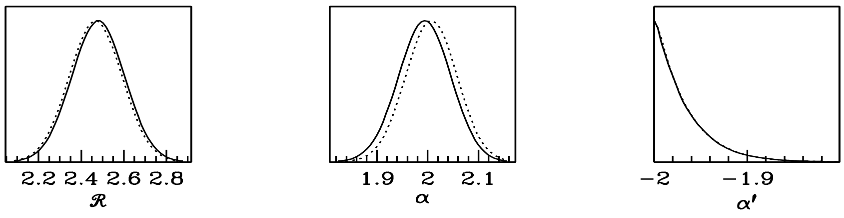

Fig. 3.— Marginalized probability density functions (pdf) of $\mathcal{R}$, α, and $\alpha\prime$, for $\beta = 0$.

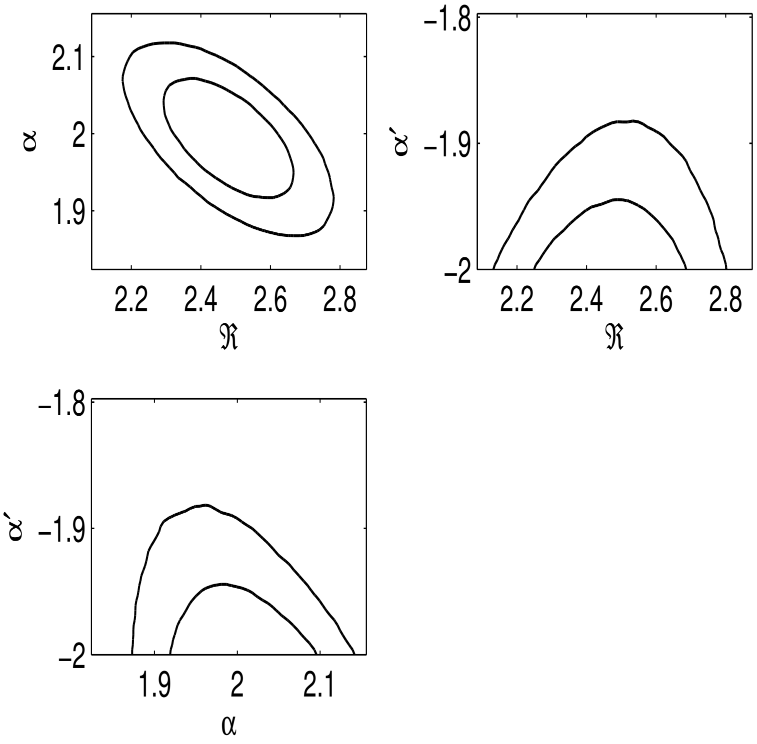

Fig. 4.— 2-D joint confidence level contours (68% and 95%) corresponding to Fig.3.

Fig.5 shows the Hubble diagrams for three cases, with the solid line indicating $m_0(z) = \mu(z) + M$ in each case, where M is obtained by minimizing the rms of $|B_{max}(z) - m_0(z)|$ (the Hubble diagram dispersion). The three cases are: (a) No corrections. (b) B_{max} corrected by subtracting $\Delta M^{cor} = \mathcal{R}E + \alpha\ (\Delta m_{15} - 1.1) + \alpha\prime\ |\Delta m_{15} - 1.1|$, with $\mathcal{R} = 2.45$, $\alpha = 2.01$, and $\alpha\prime = -2.00$. (c) B_{max} corrected by subtracting $\Delta M^{cor} = \mathcal{R}E + \alpha\ (\Delta m_{15} - 1.1) + \alpha\prime\ |\Delta m_{15} - 1.1| + \beta b_{lt}$, with $\mathcal{R} = 2.41$, $\alpha = 1.89$, $\alpha\prime = -1.45$, and $\beta = 77.49$ (mag/day)$^{-1}$. The parameter values in (b) and (c) correspond to the best fit values from the MCMC analysis (listed in Table 2). We find that including the correlation between luminosity and late-time lightcurve slope in correcting M_B^{obs} reduces the Hubble diagram dispersion from 0.14 mag to 0.12 mag.

To study the effect of the measurement uncertainty in B_{max} for our sample, we have repeated our MCMC analysis setting ΔB_{max} to a constant. This gives similar results as above. We find that including the correlation between luminosity and late-time lightcurve slope in correcting M_B^{obs} reduces the Hubble diagram dispersion from 0.13 mag to 0.11 mag. This is similar to what we find when using the actual ΔB_{max} from Table 1.

Fig.6 shows the absolute magnitude corrected for color and Δm_{15} only [case (b) of Fig.5], versus b_{lt}, with its coefficient β given by case (c) of Fig.5. This shows that the evidence for the correlation between luminosity and late-time lightcurve slope is tentative due to the small size of the sample. A much large sample of SNe Ia with well measured late-time lightcurves is needed to firmly establish this correlation.

4. Discussion and Summary

Improving the calibration of SNe Ia increases the power of SNe Ia as cosmological standard candles. We have shown the tentative evidence for a correlation between SN Ia peak luminosity and late-time lightcurve slope; brighter SNe Ia have shallower lightcurve slopes between 100-150 days from maximum light (see Fig.6). Using this correlation, we are able to reduce the intrinsic scatter of SNe Ia (measured by the Hubble diagram residue) to 0.12 mag (see Fig.5).

We use the MCMC algorithm in our likelihood analysis; this allows us to explore all the parameters simultaneously and efficiently in calibrating the SN Ia peak luminosity for our sample of SNe Ia. We only used ΔB_{max} in calculating χ^2, since including the errors in color, Δm_{15}, and late-time lightcurve slope introduces spurious pdfs in the MCMC analysis. Our results are not sensitive to the uncertainty in B_{max} (setting ΔB_{max} to a constant gives similar results to using the ΔB_{max} from Table 1). The parameter set is (M, $\mathcal{R}$, α, $\alpha\prime$, β),

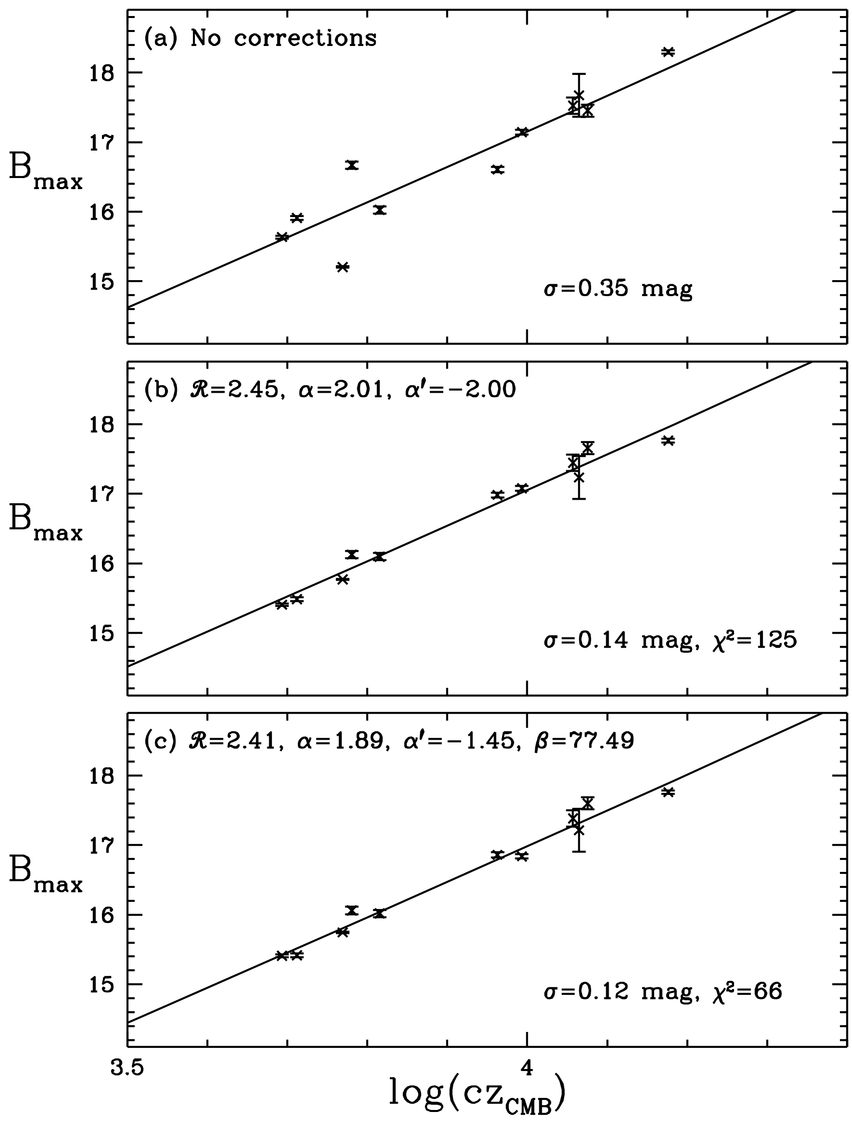

Fig. 5.— Hubble diagrams for three cases, with the solid line indicating $m_0(z) = \mu(z) + M$ in each case, where M is obtained by minimizing the rms of $|B_{max}(z) - m_0(z)|$ (the Hubble diagram dispersion). (a) No corrections. (b) B_{max} corrected by subtracting $\Delta M^{cor} = \mathcal{R}E + \alpha\ (\Delta m_{15} - 1.1) + \alpha\prime\ |\Delta m_{15} - 1.1|$, with $\mathcal{R} = 2.45$, $\alpha = 2.01$, and $\alpha\prime = -2.00$. (c) B_{max} corrected by subtracting $\Delta M^{cor} = \mathcal{R}E + \alpha\ (\Delta m_{15} - 1.1) + \alpha\prime\ |\Delta m_{15} - 1.1| + \beta b_{lt}$, with $\mathcal{R} = 2.41$, $\alpha = 1.89$, $\alpha\prime = -1.45$, and $\beta = 77.49$ (mag/day)$^{-1}$.

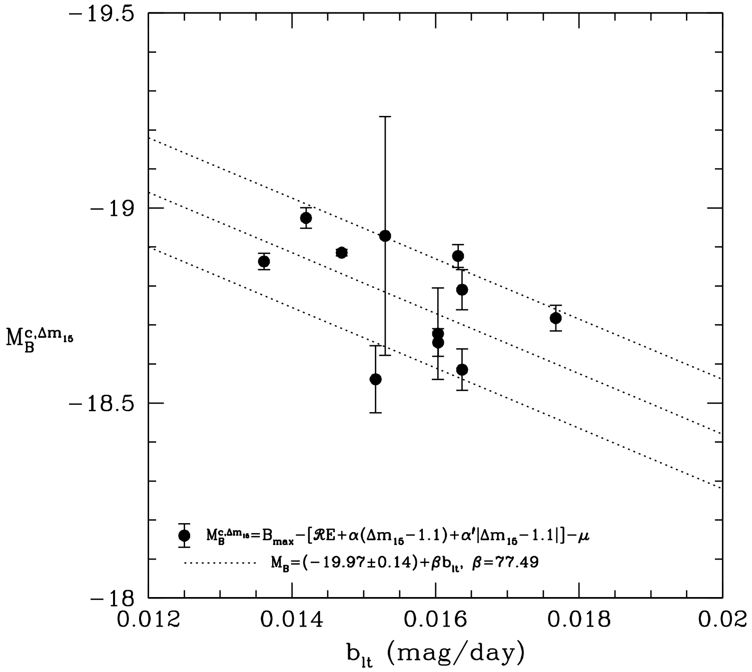

Fig. 6.— The absolute magnitude corrected for color and Δm_{15} only [case (b) of Fig.5], versus the late-time lightcurve slope b_{lt}, with its coefficient β given by case (c) of Fig.5.

which are the nuisance parameter, and correction coefficients for color, Δm_{15}, and late-time lightcurve slope respectively. The pdf's we have found for ($\mathcal{R}$, α, $\alpha\prime$, β) are very close to being Gaussian (see Fig.1 and Fig.3), except for the pdf's for $\alpha\prime$ (which are cutoff by the prior of $\alpha\prime \geq -2$). Late-time lightcurve slope b_{lt} appears uncorrelated with color (see Fig.2), which supports b_{lt} being an intrinsic observable that correlates with the peak luminosity of SNe Ia.

The coefficients for correcting for the correlation between decline-rate and peak luminosity that we have found are very different from previous work (see Table 2 and Phillips (1993); Hamuy et al. (1996a); Phillips et al. (1999); Wang et al. (2006)). This is likely partly a consequence of the particular sample of 11 SNe Ia we have used for our analysis. This is not surprising, since previous work by various groups also found very different Δm_{15} corrections (Phillips et al. 1999; Wang et al. 2006), indicating that this correction is highly sensitive to sample selection.

Note that the color correction coefficient we found was not sensitive to whether we correct for late-time lightcurve slope, and is consistent with the color correction coefficient of $\mathcal{R} = 2.59 \pm 0.24$ found by Wang et al. (2006). This is very different from a coefficient of $\mathcal{R} = 4.1$ that is typical of Milky Way dust, possibly due to the mixing of intrinsic SN Ia color variation with dust extinction (Conley et al. 2007), or variations in the properties of dust. This further strengthens the need for NIR observations of SNe Ia (Krisciunas, Phillips, & Suntzeff 2004; Phillips et al. 2006).

Our results show the benefit of extending the observations of SN Ia lightcurves beyond 100 days in the SN Ia restframe, with several data points between 50 to 150 days to enable a robust measurement of the late-time lightcurve slope. Our sample only contains 11 SNe Ia, limited by currently available data. The expansion in the scope of SN observations to obtain late-time lightcurves is straightforward for surveys which cover the same areas in the sky in regular intervals (Wang 2000; Phillips et al. 2006).

Our results have significant implications for the survey strategy of future SN surveys, such as those planned for the Advanced Liquid-mirror Probe for Astrophysics, Cosmology and Asteroids (ALPACA)[3]; Pan-STARRS[4]; the Dark Energy Survey (DES)[5]; the Large Synoptic Survey Telescope (LSST)[6], and the Joint Dark Energy Mission (JDEM).

---

[3]http://www.astro.ubc.ca/LMT/alpaca/

[4]http://pan-starrs.ifa.hawaii.edu/

[5]http://www.darkenergysurvey.org/

[6]http://www.lsst.org/

Acknowledgments We are grateful to Lifan Wang for providing the lightcurve fits to the SN data we used, Alex Conley for sending us his compilation of nearby SN data, and David Branch for helpful discussions and comments on drafts of the manuscript. This work was supported in part by the NSF CAREER grant AST-0094335 and AST 05-06028.

REFERENCES

Branch, D. 1998, ARA & A, 36, 17

Cardelli, J.A.; Clayton, G.C.; & Mathis, J.S. 1989, ApJ, 345, 245

Conley, A., et al. 2007, arXiv:0705.0367v2, ApJL, in press

Cooray, A.; Caldwell, R.R. 2006, Phys.Rev.D73, 103002

Goldhaber, G., et al. 2001, ApJ, 558, 359

Hamuy, M., et al. 1996a, AJ, 112, 2391

Hamuy, M., et al. 1996b, AJ, 112, 2408

Howell, D. A., et al. 2006, Nature 443, 308

Hui, L.; & Greene, P.B. 2006, Phys. Rev. D73, 123526

Jha, S., et al. 2006, AJ, 131, 527

Krisciunas, K.; Phillips, M.M.; Suntzeff, N.B. 2004, ApJ, 602, L81

Lewis, A., & Bridle, S. 2002, PRD, 66, 103511

Milne, P. A.; The, L.-S.; Leising, M. D. 2001, ApJ, 559, 1019

Neil, R.M. 1993, ftp://ftp.cs.utoronto.ca/pub∼radford/review.ps.gz

Perlmutter, S. *et al.*, 1999, ApJ, 517, 565

Phillips, M.M. 1993, ApJ, 413, L105

Phillips, M. M., et al. 1999, AJ, 118, 1766

Phillips, M. M.; Garnavich, P.; Wang, Y. et al. 2006, Proc. of SPIE, Volume 6265, 626529, arXiv:astro-ph/0606691v1

Press, W.H., Teukolsky, S.A., Vettering, W.T., & Flannery, B.P. 1994, Numerical Recipes, Cambridge University Press, Cambridge.

Riess, A.G., Press, W.H., and Kirshner, R.P. 1995, ApJ, 438, L17

Riess, A. G, *et al.*, 1998, Astron. J., 116, 1009

van den Bergh, S. 1995, ApJ, 453, L55

Vaughan, T. E., Branch, D., Miller, D. L., & Perlmutter, S. 1995, ApJ, 439, 558

Wang, L., et al. 2006, ApJ, 641, 50

Wang, Y.; Spergel, D.N.; & Turner, E.L. 1998, ApJ, 498, 1

Wang, Y. 2000, ApJ 531, 676

Wheeler, J. C., AAPT/AJP Resource Letter, Am. J. Phys., 71 (2003)

Woosley, S., et al. ApJ 662, 487, 2007

Zehavi, I.; Riess, A.G.; Kirshner, R.P.; & Dekel, A. 1998, ApJ, 503, 483